Technical Publications and Art Division
8265, for TIC (2)

SAND78-8675
Unlimited Release

MASTER

Hydrogen Induced Ductility Losses in Austenitic Stainless Steel Welds

J. A. Brooks, A. J. West

Sandia Laboratories

SF 2900 Q(7-73)

SAND78-8675
Unlimited Release
Printed June 1978

HYDROGEN INDUCED DUCTILITY LOSSES IN AUSTENITIC STAINLESS STEEL WELDS

John A. Brooks
Materials Science Division 8316

Anton J. West
Materials Development Division II 8314
Sandia Laboratories, Livermore

ABSTRACT

The effect of hydrogen on the tensile behavior of austenitic stainless steel welds was studied in two AISI 300 series alloys and two nitrogen strengthened alloys. The microstructure of these welds typically contained several percent ferrite in an austenite matrix. Hydrogen was found to reduce the ductility of all welds; however, the severity of ductility loss decreased with increasing stacking fault energy, as observed in previous studies on wrought material. In the lowest stacking fault energy welds, 304L and 308L, hydrogen changed the fracture mode from dimple rupture to a mixed mode of ductile and brittle fracture associated with the austenite ferrite interface. Higher stacking fault energy welds, 309S and 22-13-5, showed smaller losses in ductility. In these materials hydrogen assisted the ductile rupture process by aiding void growth and coalescence, without changing the fracture mode. Varying the amount of ferrite from approximately one to 10 percent had no significant effect on performance in hydrogen.

HYDROGEN INDUCED DUCTILITY LOSSES IN AUSTENITIC STAINLESS STEEL WELDS

Introduction

Interest in structural materials suitable for use in hydrogen environments has increased considerably in the past few years. This interest has been generated largely as a result of new energy schemes which require the production and storage of hydrogen or hydrogen containing gases[1,2]. Austenitic stainless steels, in spite of their high cost and strength limitations, have received considerable attention for severe hydrogen applications because they are relatively little affected by hydrogen[3-14]. However, most studies on the effects of hydrogen on austenitic stainless steels deal with wrought material; little work has been done on welds. This becomes somewhat alarming when one considers that virtually every structural application for hydrogen generation or storage includes welds. It may be expected that second phases and chemical segregation present in welds would result in considerably different behavior of welds compared to wrought material when subjected to hydrogen environments, so that prediction of weld behavior in hydrogen from data on wrought material would be risky.

In an earlier study on 304L welds, we showed that for tensile tests conducted in 69 MPa hydrogen, fracture initiated and propagated along ferrite stringers of the weld fusion zone.[15] This behavior was contrasted to samples tested in air where fracture occurred by void growth and coalescence. The observation of fracture along or near the ferrite-austenite boundary raises the question as to whether the fracture mechanism in hydrogen is: (1) embrittlement of the BCC ferrite by hydrogen, (2) reduction of the boundary cohesive energy due to impurity segregation and hydrogen-impurity interactions[16], or finally (3) hydrogen-assisted fracture due to a local pressure buildup caused by the transport of hydrogen with dislocations to the ferrite-austenite interface.[11,17,18] One goal of the present study is to determine which of these mechanisms, if any, controls the behavior of austenitic stainless steel welds in hydrogen.

The study compares the hydrogen susceptibility of two AISI 300 series alloys, 304L (19Cr-11Ni-.02C) and 309S (23Cr-14Ni-.06C), with two higher-strength nitrogen-bearing alloys, 21-6-9 (21Cr-6Ni-9Mn-.3N) and 22-13-5 (22Cr-13Ni-5Mn-.3N). Weld deposits in these alloys usually contain some ferrite to prevent weld cracking. The amount of ferrite in the weld deposit can vary considerably from heat-to-heat. The importance of ferrite in preventing weld cracking has led to the development of diagrams used to predict weld ferrite content from alloy composition. By plotting the allowable AISI composition ranges for 304L and 309S on the DeLong diagram,[19] it can be seen that welds in these alloys can contain any amount of ferrite from little or none to nearly 20 percent (Figure 1). However, ferrite levels greater than

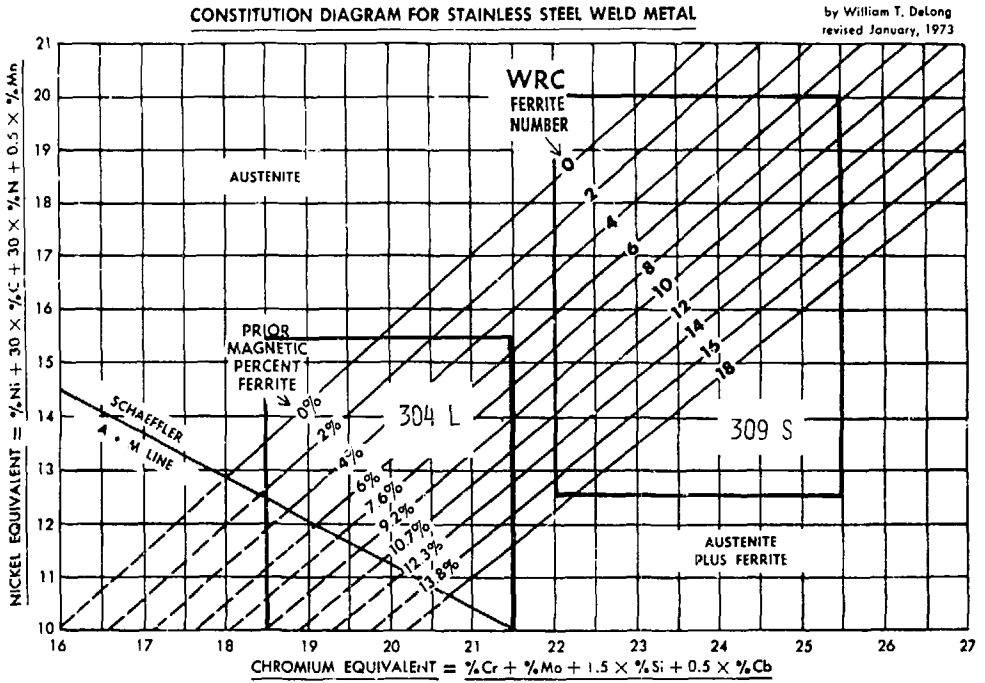

Figure 1. DeLong Diagram showing the allowable ranges in weld ferrite within the AISI composition specification of 304L and 309S. The approximate relationship between ferrite number (FN) and percent ferrite is also shown.

~15% are rather uncommon due to the unlikely occurrence of all austenite-forming elements being at the minimum level and all ferrite forming elements being simultaneously at the maximum level. Furthermore, ferrite levels are often limited to maintain high ductility during ingot breakdown and fabrication at elevated temperatures. The diagram developed by Hull[20], unlike the DeLong diagram, is accurate in predicting ferrite levels of the higher manganese, nitrogen strengthened alloys like 21-6-9 and 22-13-5. Welds in these alloys can also cover a large range in ferrite content[21].

The four alloys used in this study provide a good basis from which to study the role of ferrite on the hydrogen embrittlement of welds since, while comprising a large range in overall chemical composition, they still all contain ferrite in the weld deposit. Also, small changes in composition producing large changes in ferrite content could be made to study the effect of ferrite content on hydrogen embrittlement.

Experimental Procedure

Back extruded high energy rate forged cylinders approximately 10 cm in diameter with a 1.5 cm wall thickness were fabricated from commercial heats of 304L, 21-6-9 and 22-13-5 bar stock. These cylinders were machined and welded by two different processes: gas tungsten arc (GTA) and electron beam cold wire feed (EBCW). The GTA process utilized a much wider U-groove than that for the EBCW process and consequently has a much wider fusion zone, Figure 2. Tensile samples with a 5 mm gage diameter and 25.4 mm gage length were machined from the center of the cylinder wall with the weld fusion zone located at the center of the gage length. These specimens contained the parent material, fusion zone and heat-affected zone and therefore the yield strength and elongations are representative of the composite specimen. However, all welds broke in the fusion zone and thus the ultimate tensile strength and the reduction in area (RA) are truly weld metal properties.

Welds were also made in 304L and 309S plates which produced different amounts of ferrite in the weld deposit. It was desired to change only the ferrite content of the welds and keep changes in material composition, impurity concentrations and welding conditions at a minimum. To do this, small amounts of either nickel or chromium were electroplated on the edge of annealed plates which were subsequently butt welded using the GTA process. Several autogeneous weld passes were made in an attempt to produce uniform mixing. Chromium electroplate was used to increase ferrite content in 309, while nickel was used to decrease the level of ferrite in 304L. The DeLong diagram (Figure 1) predicts that an increase of 1% nickel results in a 2-3% decrease in ferrite, while an increase in 1% chromium results in ~3% increase in ferrite content. The ferrite levels were measured with a mage gage and reported as ferrite number (FN). As shown in Figure 1, below ~10% ferrite level, FN is approximately equal to the percent of ferrite in the weld deposit. For welds in which ferrite level was varied, notched specimens were used to force fracture to occur in the welds. In this case, the 45° notch with a 3.95 mm diameter and 1.3 mm radius was placed in the center of the fusion zone. The surfaces of all samples were polished with 400 grit silicon carbide paper,

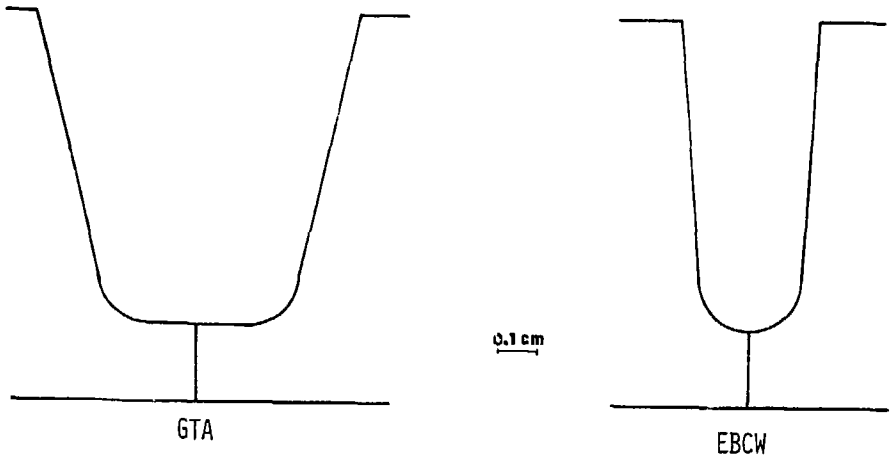

Figure 2. Weld joint geometrics of 1.5 cm wall thickness cylinders showing the much wider grove used for the GTA process compared to that of the EBCW process.

to remove ~25 microns of the machined surface, and rinsed in alcohol before testing or thermal charging with hydrogen.

Tensile specimens were thermally charged in 24 MPa hydrogen at 473°K for ten days. These charging conditions result in a hydrogen concentration profile which simulates long term exposures. The resulting hydrogen profile, shown elsehwere for austenitic stainless steels[18], is ~2500 atm ppm at the specimen surface decaying to ~200 atm ppm in the center. The predicted hydrogen profile neglects any contributions from the ferrite. The hydrogen charged samples were tested in either 69 MPa hydrogen or air at a strain rate of 3.3×10^{-4} sec^{-1}. Uncharged samples were also tested in 69 MPa hydrogen. Duplicate samples were tested and compared. In addition to tensile testing, the failed welds were examined in the scanning electron microscope to characterize the fracture mode.

Results

The properties of 304L/308L (304L base material joined with 308L filler wire) GTA welds are shown in Table I. As shown, these welds exhibit extensive work hardening and good ductility. When tested in 69 MPa hydrogen the tensile properties were essentially unchanged except for a 16% loss in RA. Thermal charging had a larger effect on tensile ductility than did testing in 69 MPa hydrogen. In thermal charged samples, the uniform and total elongations were reduced ~11% and ~26% respectively, and the RA reduced ~31%. The combined effect of thermally charging and testing in 69 MPa hydrogen produced the largest ductility losses. In this condition the uniform and total elongation were reduced 27% and 30% respectively and the RA reduced 36%. Hydrogen had no effect on the yield or ultimate tensile strength for any conditions tested.

The fracture mode of the 304L/308L GTA welds in the uncharged air tested condition is shown in Figure 3. The fracture is completely ductile, occurring by microvoid growth and coalescence. No evidence of the weld microstructure, such as the solidification structure or delta ferrite morphology was observed on the fracture surface. This ductile fracture appearance is representative of all welds which were tested in air in the uncharged condition.

Figure 4 shows the microstructure and fractography of the 304L/308L GTA welds tested in 69 MPa hydrogen after thermal charging. A large portion of the fracture surface exhibits a dendritic appearance and severe secondary cracking (Figure 4a). The higher magnifications (Figures 4b, c) reveal a relatively brittle fracture mode - a significant change from the dimple ductile fracture of hydrogen-free welds. Figure 4d shows the underlying weld microstructure near the fracture surface. As shown, fracture occurred along the ferrite stringers. However, it can not be clearly distinguished whether the fracture path is along the ferrite-austenite interface or in the ferrite or austenite structures themselves. Regions further from the surface exhibited increasingly more ductile behavior, and near the center of the specimen fracture was completely dimple rupture.

Tensile properties of 21-6-9 GTA and EBCW welds with both 308L and 21-6-9 filler wire are shown in Table 2. The yield and ultimate tensile

Table 1

304L/308L GTA WELD PROPERTIES

Specimen Condition	0.2%YS (MPa)	UTS (MPa)	El_u (%)	El_T (%)	RA (%)	RA Loss (%)
Unc/Air	395.8	619.2	16.8	23.2	64.0	
Unc/69 MPa H_2	409.9	621.9	18.0	22.8	54.0	16.0
C/Air	409.6	626.8	14.9	17.2	44.0	31.0
C/69 MPa H_2	425.8	615.7	12.2	16.1	41.0	36.0

C = 10 day charge at 24 MPa H_2 and 473°K
2.54 cm gage length

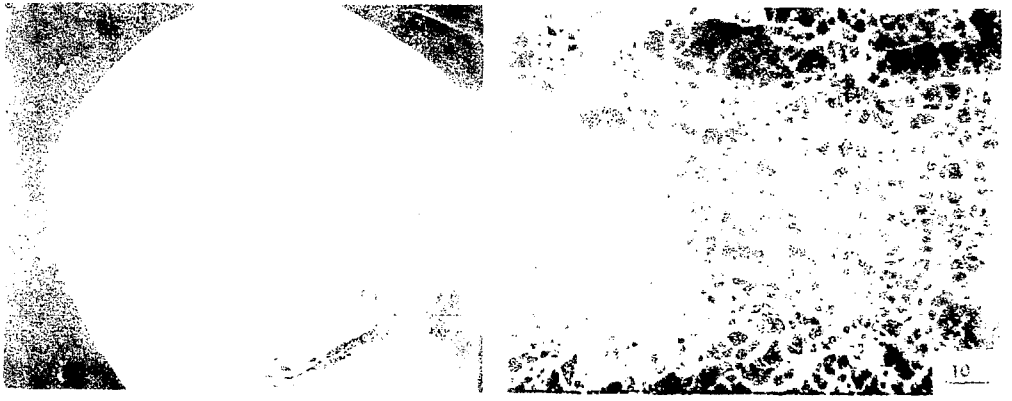

Figure 3. Fractography of 304L/308L GTA weld uncharged tested in air. This fracture behavior is typical of all uncharged, air tested welds.

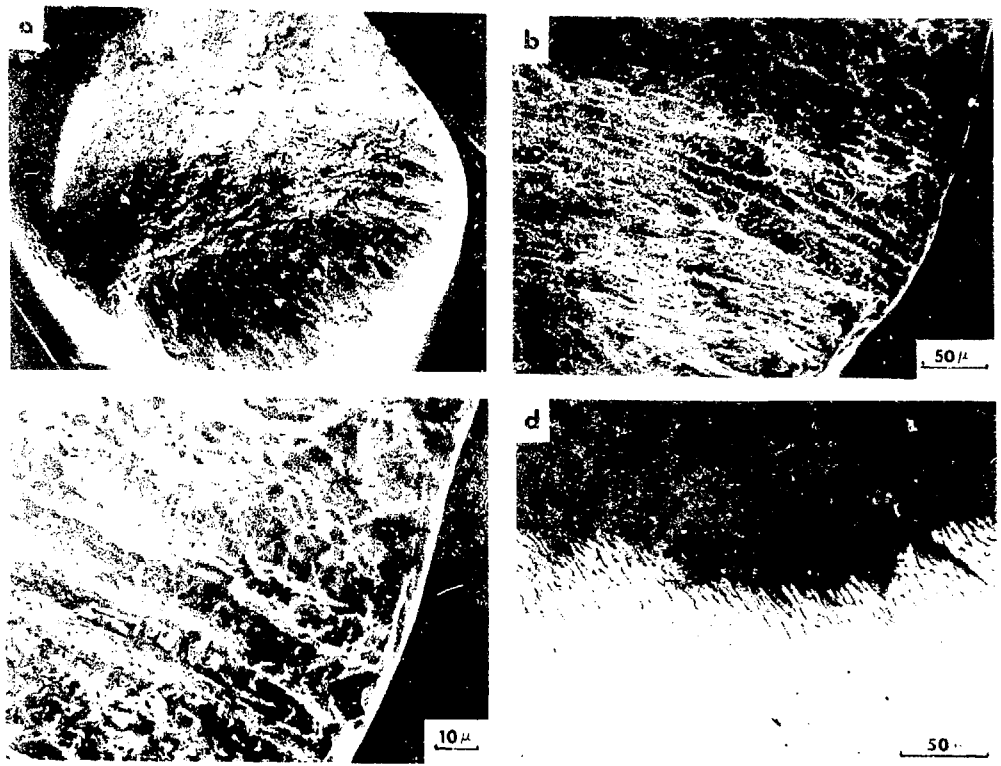

Figure 4. Fractrography of 304L/308L GTA welds thermally charged and tested in 69 MPa hydrogen. Fracture is related to ferrite, shown in (d).

Table 2

21-6-9 WELD PROPERTIES

		0.2%YS (MPa)	UTS (MPa)	El_U (%)	El_T (%)	RA (%)	RA Loss (%)
GAS TUNGSTEN ARC WELD							
308 Filler	Unc/Air	464.1	737.1	33.5	43.8	61.6	
	C/69 MPa H_2	484.8	756.4	35.2	36.9	43.3	30
21-6-9 Filler	Unc/Air	576.5	818.5	25.5	38.6	57.2	
	C/69 MPa H_2	611.6	826.8	23.0	25.1	50.2	12
EBCW WELD							
308 Filler	Unc/Air	626.8	806.8	21.0	30.5	58.2	
	C/69 MPa H_2	642.6	859.9	22.5	25.0	46.7	20
21-6-9 Filler	Unc/Air	650.2	827.4	21.6	32.5	58.2	
	C/69 MPa H_2	655.8	820.6	21.1	24.5	51.0	12

C = 10 day charge at 24 MPa H_2 and 473°K
2.54 cm gage length

strengths of GTA welds with 21-6-9 filler are higher than those with 308L filler, but have less elongation. For both filler metals, the UTS and uniform elongation were unchanged when thermally charged and tested in hydrogen. However, charging and testing in hydrogen resulted in a reduction in total elongation to a level only a few percent higher than the uniform elongation. The RA was also reduced: 30% for welds made with 308L, but only 12% for 21-6-9 filler welds.

The EBCW welds had equivalent strength for both filler wires and a 60-160 MPa higher composite yield strength than the GTA welds. This increased yield strength is a result of the narrow weld zone of the EBCW welds. In the narrow welds a smaller fraction of the lower strength weld zone is contained within the 2.54 cm gage length than for the GTA welds. The remaining material within the gage length is comprised of the higher strength forged base material. The constraint of the narrow lower strength weld zone by the higher strength base material also contributes to the higher measured yield strengths of the EBCW welds. The UTS of the EBCW 308L welds was also about 80 MPa higher than the 308L GTA welds. This again results from the increased constraint of the narrow lower strength 308L weld zone by the higher strength base material. The yield and ultimate strengths, and uniform elongation of all the EBCW welds were unaffected by hydrogen; however, the total elongations were reduced ~20% for both filler wires, but the loss in RA was again higher for the 308L filler welds than those of 21-6-9 (20% vs. 12%).

The fractography of 21-6-9/21-6-9 GTA welds thermally charged and tested in hydrogen is shown in Figure 5. The fracture contains both a flat region and a large shear section. The flat section contains some secondary cracking. Regions of the primary fracture near the outer surface of the specimen (Figure 5b) exhibits a less ductile fracture appearance than the center of the specimen where the hydrogen concentration is lowest and dimple rupture occurred (Figure 5c). The near surface region still exhibited areas of very fine dimples and more ductile fracture than the 304L/308L welds. The weld cross-section (Figure 5d) shows that both surface cracking and secondary cracking is associated with weld ferrite. The fracture appearance of 21-6-9/308L GTA welds was similar to those made with 21-6-9 filler but exhibited a higher percentage of hydrogen-affected fracture region. However, the regions which exhibited a fracture mode change due to hydrogen were still significantly less than that of the 304L/308L welds.

The fracture characteristics of EBCW welds made with 308L wire are shown in Figure 6. Here also secondary fracture associated with weld microstructure resulted when samples were charged and tested in hydrogen. Regions near the edge of the samples exhibited a quasi-cleavage fracture appearance. At the center of the specimen (still in the regions of secondary fracture) fracture was ductile and exhibited a very fine dimple size. The fracture characteristics of the 21-6-9/21-6-9 EBCW welds were similar to the 308L filler welds.

The preceeding results suggest that hydrogen assisted fracture is associated with the ferrite-austenite boundary. As described in the preceeding section, welds of varying ferrite level were tested to determine the influence of ferrite content on weld mechanical properties in hydrogen. The notched tensile properties of 304L and 309S containing ferrite levels

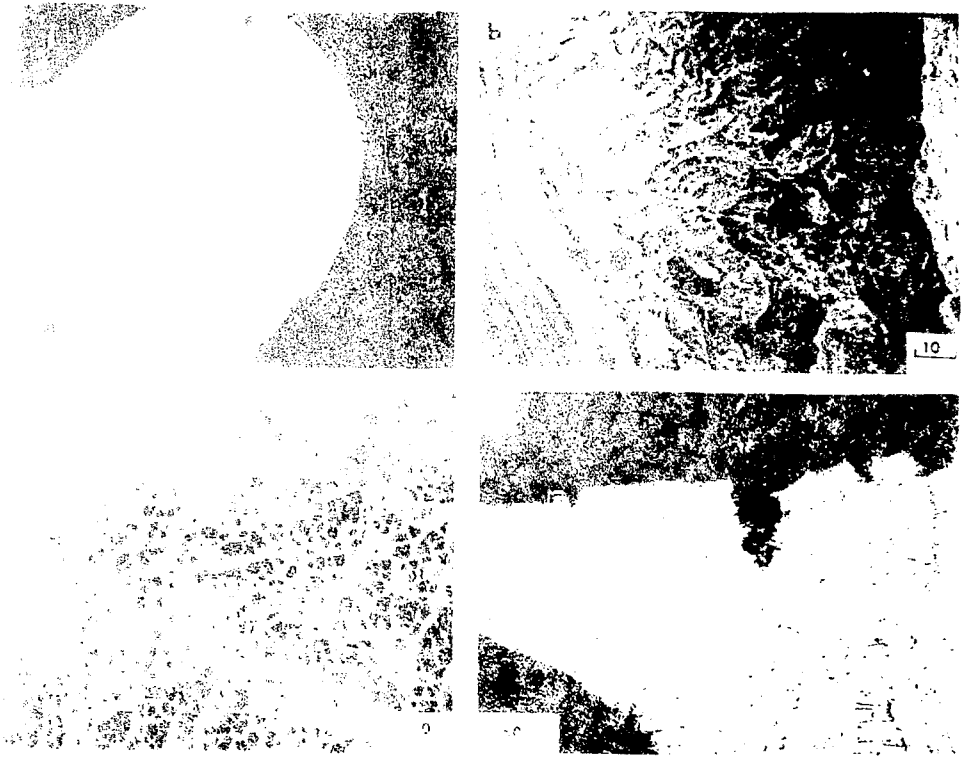

Figure 5. Fractography of 21-6-9/21-6-9 GTA welds thermally charged and tested in 69 MPa hdyrogen. Note in (d) surface cracking and secondary fracture associated with ferrite.

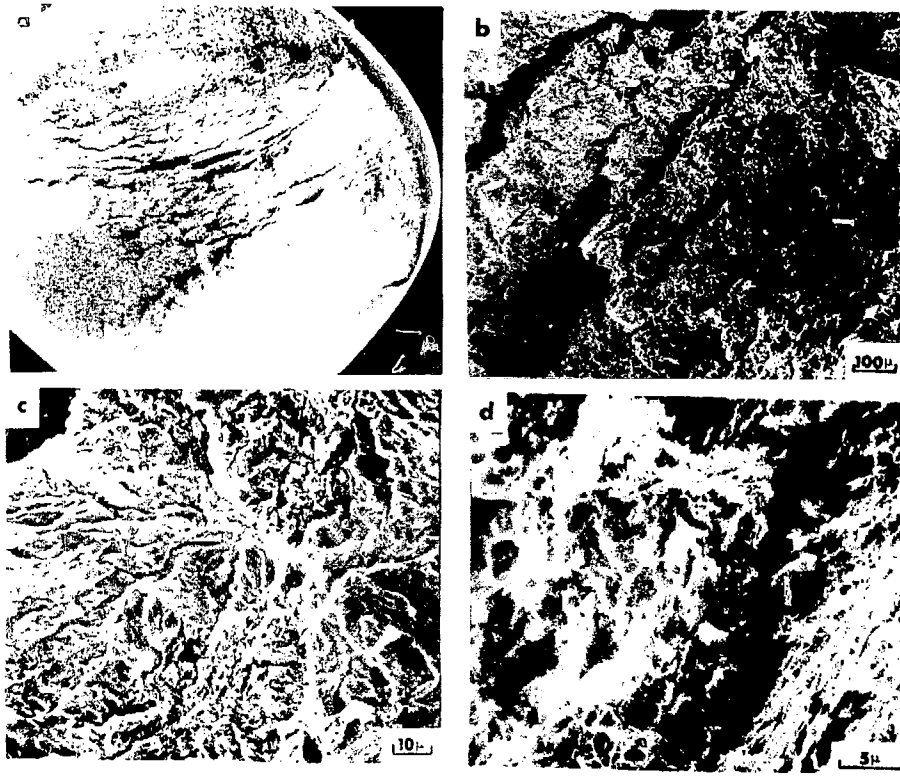

Figure 6. Fractography of 21-6-9/21-6-9 GTA welds thermally charged and tested in 69 MPa hydrogen. Center of specimen shown in (b) and (d), edge (c).

from 1 to 10% are shown in Table 3. Increasing the ferrite level in 304L welds from 4.7 FN to 8.5 FN resulted in a 23% increase in notched tensile strength with no corresponding decrease in RA. Thermal charging and testing 304L welds in 69 MPa hydrogen resulted in both a loss in tensile strength (10% loss for 4.7 FN and 17% loss for 8.5 FN) and a 60% loss in RA.

Increasing the ferrite content of 309 from 1.2 to 11.5 FN resulted in about a 10% increase in notched tensile strength, the same as for 304L. This increase in strength was accompanied by a loss in RA of approximately 24%. Thermal charging and testing in hydrogen resulted in a slight increase in strength at low ferrite levels, unlike 304L where the strength was reduced by hydrogen. Like 304L, the loss in RA due to hydrogen was independent of ferrite content; however, the loss in RA averaged only ~15% compared to ~60% for the 304L weld samples.

The fracture mode of the notched 304L and 309S welds when tested in air was again completely ductile dimple rupture. When thermally charged and tested in hydrogen, fracture of the 304L welds occurred predominately along the ferrite-austenite interfaces as in the 304L/308 welds. Fracture of the 309S welds was unaffected by hydrogen and completely ductile except for several isolated areas very near the surface. Contrasting fracture surfaces of the 304L and 309S welds when tested in hydrogen are shown in Figure 7.

The 22-13-5 GTA weld properties are shown in Table 4. No loss in tensile ductility was observed when tested in 69 MPA hydrogen. Thermal charging and testing in air, however, did produce some losses in ductility. In comparing these results with the uncharged air properties the uniform and total elongation were reduced about 14 and 24% respectively. The RA was also reduced 23%. Examination of the fracture surface showed that fracture occurred by dimple rupture and was unchanged by hydrogen, as observed in the 309S welds.

Discussion

The behavior of the weld deposits in the presence of hydrogen varied widely with alloy chemical composition. However, a good correlation was found to exist between "average" stacking fault energy (SFE) and RA loss due to thermal charging and testing the GTA welds in hydrogen (Figure 8). The values for SFE were taken from studies on base material by Schram and Reed[22]. The absolute values of SFE may be in question but we think the relative ranking is correct. The "average" SFE of the 21-6-9/308L weld was calculated based on a 50-50 mixture of the base and filler material. A similar relationship between SFE and RA loss has been observed for the single phase austenitic stainless steel base metal[14]. This relationship can be explained mechanistically by the transport of hydrogen by dislocations[11,23,24]. In low SFE materials, where planar slip occurs over large amounts of strain, high concentrations of hydrogen can be deposited at internal boundaries by dislocations moving on well defined slip planes. Hydrogen at the boundaries can accelerate the fracture process by a number of mechanisms, such as a pressure build-up or a reduction in cohesive strength of the boundary. In welds, these boundaries may be the ferrite stringers as well as grain boundaries. In the case of the low SFE welds, i.e., 304L and 308L, transport of

Table 3

EFFECT OF FERRITE ON HYDROGEN PROPERTIES OF
304L AND 309 WELDS - NOTCHED TENSILES

Alloy	% Ferrite (FN)	Condition	UTS (MPa)	RA (%)	RA Loss (%)
304L	4.7	Unc/Air	726.8	39.5	-
		69 MPa H_2	657.8	14.4	64
304L	8.5	Unc/Air	893.6	39.5	-
		69 MPa H_2	739.8	17.0	57
309S	1.2	Unc/Air	714.3	27.9	-
		69 MPa H_2	741.9	25.5	8
309S	8.5	Unc/Air	742.6	23.5	-
		69 MPa H_2	751.6	17.4	23
309S	11.5	Unc/Air	782.6	21.3	-
		69 MPa H_2	780.5	18.2	15

C = 10 day charge at 24 MPa H_2 and 473°K

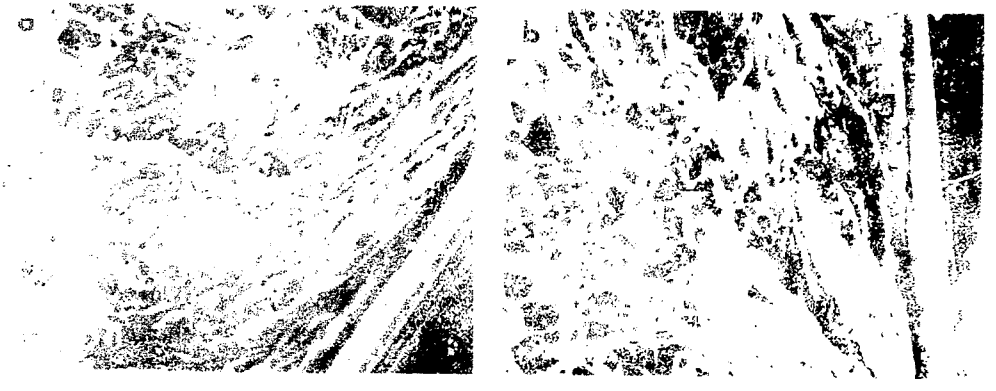

Figure 7. Fracture surfaces of the high ferrite welds charged and tested in hydrogen. (a) 304L (FN 4.7), fracture associated with the weld ferrite (b) 309S 11.5 FN fracture mode unchanged by hydrogen.

Table 4

22-13-5/22-13-5 GTA TENSILE PROPERTIES

Specimen Condition	0.2%YS (MPa)	UTS (MPa)	El_U (%)	El_T (%)	RA (%)	RA Loss (%)
Unc/Air	495	782	11.2	14.4	49.2	-
Unc/69 MPa H_2	511	778	13.0	16.3	48.5	1.4
C/Air	511	790	9.6	10.9	38.0	23.0
C/69 MPa H_2	531	776	10.2	12.0	44.5	10.0

C = 10 day charge at 24 MPa H_2 and 473°K
2.54 cm gage length

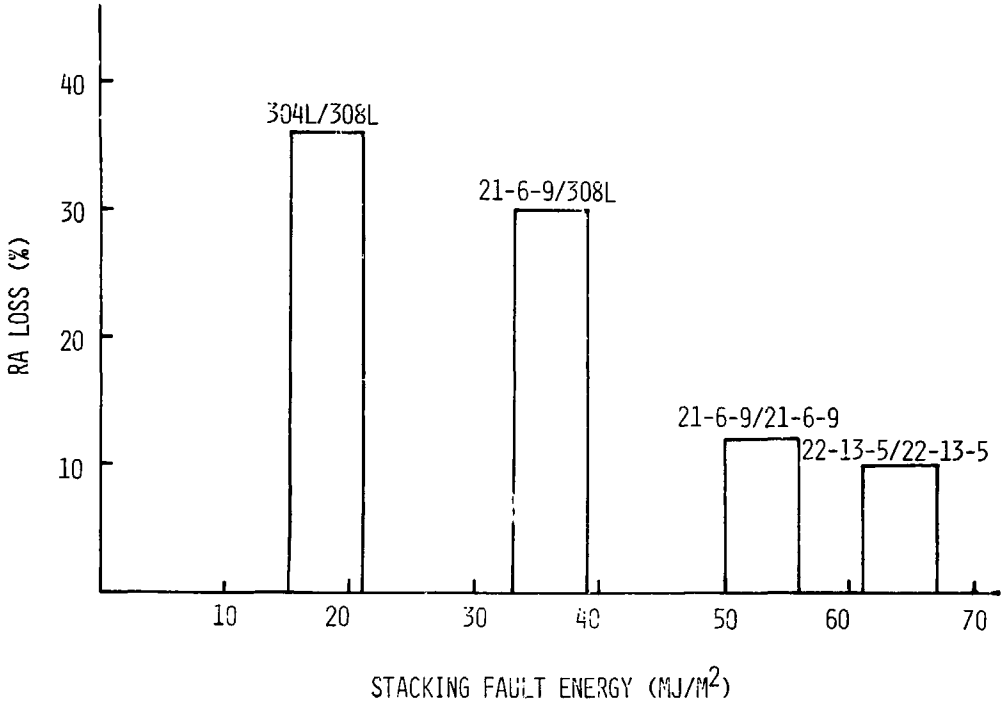

Figure 8. SFE vs RA loss for GTA welds thermally charged and tested in hydrogen.

hydrogen to these internal boundaries was sufficient to result in a change in fracture location from transgranular dimple rupture in the absence of hydrogen to fracture along the ferrite boundaries in the presence of hydrogen. At regions near the center of the sample where the hydrogen concentration was lowest, the fracture remained predominantly dimple rupture, but the dimple size was considerably smaller than that of the hydrogen free samples. This change in dimple size has been attributed to hydrogen assisting the ductile fracture process.[8] In the proposed rationale, during plastic deformation hydrogen is deposited at inclusions where it may either reduce the interface strength or stablize small voids, and subsequently aid void growth by internal pressure. Thus, at the center of the sample the hydrogen concentration near the ferrite-austenite interface never reaches a sufficient level to produce a change in fracture mode from dimple rupture to interfacial separation. In higher SFE welds, the fracture mode change is confined to regions nearer the surface where the hydrogen concentrations are highest, this was the case in the 21-6-9/308L and 21-6-9/21-6-9 welds. In the 309 and 22-13-5 the critical hydrogen concentrations required for fracture at the ferrite-austenite interface was never achieved with the testing conditions used in this study. For these welds, the losses in ductility are due entirely to the hydrogen assist on the ductile rupture process as indicated by the absence of a fracture mode change in hydrogen.

Extensive and detailed fractography of the 304L and 304L/308L welds tested in hydrogen suggest that fracture associated with ferrite occurred mainly along the ferrite-austenite interface, rather than through the ferrite. The fracture surface of a 304L/308L weld charged and tested in hydrogen, shown in Figure 9, exhibits areas that are smooth and indicative of interface separation, rather than cleavage as would be expected if fracture occurred in the ferrite at these severe testing conditions. This is in agreement with our earlier studies on 304L welds in which fracture also appeared to occur at the interface [15]. The 309 and 22-13-5 welds did not exhibit any fracture related to ferrite even very near the surface where the concentration of hydrogen due to the combined effect of charging and testing in 69 MPa hydrogen is very high. At these hydrogen levels, it would seem that the ferrite structure would be sufficiently embrittled to result in some fracture mode changes, even with only a limited contribution from hydrogen transport to the ferrite structure. The absence of an observed fracture mode change, even in the severe case of the notched 309S welds, lends credence to the mechanism by which the transport of large amounts of hydrogen to the ferrite-austenite interface results in fracture along the interface rather than through the ferrite structure. Whether or not impurities segregated to the boundaries during welding interact with hydrogen to weaken the boundaries is not known, but no evidence for such was observed by Auger spectroscopy studies on the fracture surfaces. In the 21-6-9 welds, sufficient hydrogen transport appeared to cause fracture to initiate at the ferrite-austenite interface. However, the more ductile appearing fracture along the ferrite-austenite interfaces of these welds suggest that the quantities of hydrogen are lower than for 304L. This is in agreement with what may be expected for 21-6-9 welds with SFE between that of 304L and 309.

The RA losses in 304L welds are similar to those of base material [16]. In 304L base material, the fracture mode is also changed by hydrogen from ductile rupture to intergranular fracture. Since the ferrite itself is

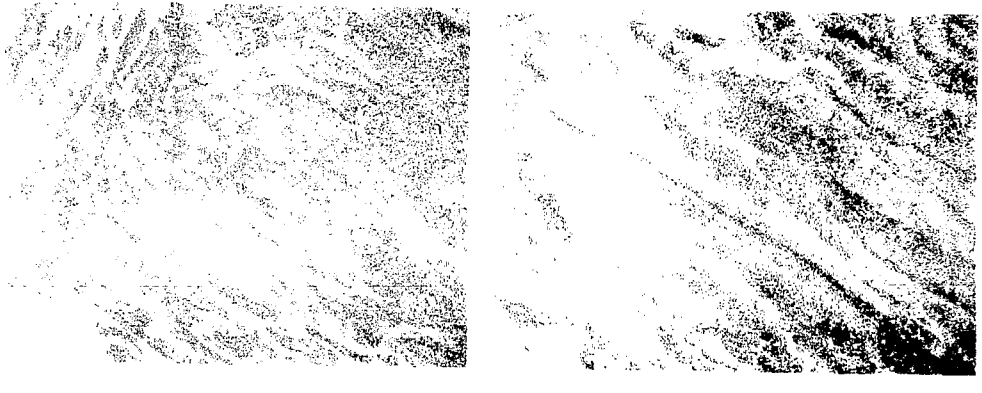

Figure 9. Fracture of 304L/308L GTA weld charged and tested in 69 MPa hydrogen. Smooth fracture features indicative of failure along the ferrite-austenite interfaces.

not embrittled in welds, no dependence was found to exist between the quantity of ferrite in the 304L welds and the degree of ductility loss due to hydrogen. The stringer like morphology of ferrite evidently produces a sufficiently large area of interfacial boundary, even at low levels of ferrite, for hydrogen to accumulate and accelerate the fracture process. The independence of ferrite content on the loss in RA of 309 welds is even less surprising since fracture is not associated with ferrite.

Summary

The effect of hydrogen on the tensile ductility of austenitic stainless steel welds was studied using two AISI 300 series alloys (304L and 309S), and two nitrogen strengthened alloys (21-6-9 and 22-13-5). Tests of the effects of thermal charging and high pressure (69 MPa) hydrogen were conducted on GTA and EBCW welds. All welds exhibited some loss in ductility due to hydrogen. Their behavior is consistent with models for transport of hydrogen by dislocations to localized regions in the structure where hydrogen deposition can affect the fracture process. For the high SFE welds, i.e., 309S and 22-13-5, in which hydrogen transport is least efficient, the small losses in ductility resulted solely from hydrogen assisting the ductile fracture process. In the low SFE welds, i.e., 304L and 308L, sufficiently high concentrations of hydrogen were transported to the ferrite-austenite interface that in many regions fracture no longer occurred by a transgranular ductile dimple process, but rather by interphase separation. In the 21-6-9 welds sufficient hydrogen transport resulted such that fracture occurred along the ferrite-austenite interface; however, the fracture mode was more ductile than for the 304L welds. It is likely that in the 304L welds high concentrations of hydrogen resulted in interface separation rather than brittle fracture of the BCC ferrite. In both 304L and 309S varying the ferrite content from a few to approximately ten percent had no effect on hydrogen susceptibility.

Acknowledgment

The authors are greatful for the experimental assistance of D. Clark, A. Salmi, and J. O'Connor, and the scanning electron microscopy conducted by C. Karfs, and the optical metallography by T. Bryant.

References

1. K. E. Cox, Effect of Hydrogen on Behavior of Materials, pp. 3-17, 1976.

2. A. L. Hammond, W. D. Metz, and T. A. Maugh, Energy and the Future, pp. 11-23, 117-123 A.A.A.S., Washington, 1973.

3. A. R. Troiano, Trans. ASM, Vol. 52 pp. 54-80, 1960.

4. R. M. Vennett and G. S. Ansell, Trans. ASM, Vol. 60 pp. 242-251, 1967.

5. R. M. Vennett and G. S. Ansell, Trans. ASM, Vol. 62 pp. 1007-13, 1969.

6. R. J. Walter and W. T. Chandler, Effects of High Pressure Hydrogen on Metals at Ambient Temperatures, Report R-7780-1. Rocketdyne Division Rockwell International, Feb. 1969.

7. R. J. Walter, R. P. Jewett, and W. T. Chandler, Mater. Science Engr. Vol. 5, pp. 99-110, 1969-70.

8. A. W. Thompson, Hydrogen in Metals, ASM, pp. 91-102, 1974.

9. M. R. Louthan, Hydrogen in Metals, ASM, pp. 53-75, 1974.

10. H. J. Saxton, A. J. West, and A. W. Thompson, Effect of Hydrogen on Behavior of Materials, ASM, pp. 631-641, 1976.

11. M. R. Louthan, G. R. Caskey, J. A. Donovan, and D. E. Rawl, Mater. Sci. Engr. Vol. 10, pp. 357-368, 1972.

12. A. W. Thompson, Met. Trans., Vol. 4, pp. 2819-25, 1973.

13. A. W. Thompson, Mater. Sci. Engr., Vol. 14, pp. 253-64, 1974.

14. B. C. Odegard, J. A. Brooks, and A. J. West, Effect of Hydrogen on Behavior of Materials, ASM, pp. 116-125, 1976.

15. A. J. West, J. A. Brooks, Effect of Hydrogen on Behavior of Materials, ASM pp. 686-697, 1976.

16. C. J. McMahon, C. L. Briant, and S. K. Bauerji, Fracture 1977, Vol. I, Waterloo, Canada, June 19-24, 1977, pp. 363-385.

17. A. W. Thompson, B. A. Wilcox, Scr. Met., 1972, Vol. 6, pp. 689-96.

18. A. W. Thompson, J. A. Brooks, Met. Trans., Vol. 6A, p 1442, 1975.

19. W. DeLong, G. Ostrom, E. Szumachowski, Welding J. Vol. 35 (11) Nov. 1956, Res. Suppl. 521-s to 528-s.

20. F. C. Hull, Welding J. Vol. 52(5) 1973, Res. Suppl. 193-S to 203-S.

21. J. A. Brooks, Weld J. Vol. 52(6) 1975, Res Suppl. 189-S to 195-S.

22. B. E. Schramm and R. P. Reed, Met. Trans., 1975, Vol. 6A, pp. 1345-51.

23. P. Bastien and P. Azou C. R. Acad. Sci. Paris, 1951 vol. 232, pp. 1845-48.

24. J. K. Tien, A. W. Thompson, I. M. Berstein, and R. J. Richards. Met. Trans., Vol. 7A pp. 821-829, 1976.